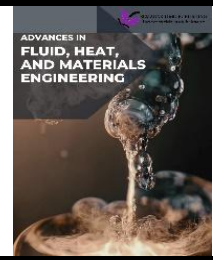




## Advances in Fluid, Heat and Materials Engineering

Journal homepage:  
<https://semarakilmu.com.my/journals/index.php/afhme/index>  
ISSN: 3083-8134



# CFD Analysis of Coronavirus Dispersion through Breathing in Aircraft Cabin Environments

Asral<sup>1</sup>, Ridwan Abdurrahman<sup>1</sup>, Khoo Wai Chang<sup>2</sup>, Ishkriyat Taib<sup>2,\*</sup>, Nur Amani Hanis Roseman<sup>2</sup>, Kong Kar Hoe<sup>2</sup>, Lee Cheng San<sup>2</sup>, Khairul Shafaiz Bin Jesni<sup>2</sup>, Awaludin Martin<sup>1</sup>

<sup>1</sup> Department of Mechanical Engineering, Universitas Riau, Pekanbaru, 28293, Indonesia

<sup>2</sup> Faculty of Mechanical and Manufacturing Engineering, Universiti Tun Hussein Onn Malaysia, Batu Pahat, 86400, Malaysia

### ARTICLE INFO

#### Article history:

Received 23 March 2024

Received in revised form 30 April 2024

Accepted 5 June 2024

Available online 21 June 2024

#### Keywords:

Coronavirus; COVID-19; breathing; simulation; computational fluid dynamic; air cabin; flow characteristics; velocity; pressure

### ABSTRACT

In 2019, the coronavirus rapidly spread worldwide and was declared a pandemic by the World Health Organization (WHO). As the world is currently in the post-COVID stage, many sectors, including air travel, are being reopened. To understand the flow characteristics in aircraft cabins due to the breathing of a coronavirus patient, a simulation was conducted using Computational Fluid Dynamics (CFD). In this study, a simplified 7-row commercial aircraft cabin was modelled. In addition, a human manikin was designed to simulate the breathing of a coronavirus patient in the cabin. The simulation was conducted using ANSYS Fluent with an inlet velocity of 1 m/s for the cabin air, an outlet pressure of 84,475.3 Pa, and a human breathing velocity of 1.3 m/s. The results showed that the breathing of a coronavirus patient could affect passengers seated up to three rows in front of the patient on both sides of the cabin. Further research is needed to consider other factors that can influence the flow characteristics of a coronavirus patient's breath, such as temperature, humidity, and other velocity ranges.

## 1. Introduction

An outbreak of mysterious pneumonia characterised by fever, dry cough, fatigue, and occasional gastrointestinal symptoms was discovered at The Huanan Seafood Wholesale Market in Wuhan, Hubei, China in late December 2019 [1]. The outbreak affected approximately 66 percent of the workers. After the local health authority issued an epidemiologic alert on 31 December 2019 the market closed on 1 January 2020. Unfortunately, thousands of people in China, including many provinces such as Hubei, Zhejiang, Guangdong, Hunan, and cities such as Beijing and Shanghai, were affected by the rapid spread of the disease in the following month. To make matters worse, the disease has spread to other countries, such as Thailand, Japan, the Republic of Korea, Vietnam, Germany, the United States, and Singapore.

\* Corresponding author.

E-mail address: [iszat@uthm.edu.my](mailto:iszat@uthm.edu.my)

<https://doi.org/10.37934/afhme.1.1.4959>

The first case of COVID-19 was detected in Malaysia on 25 January 2020 and was traced back to three Chinese nationals who had previously had close contact with an infected person in Singapore [2]. Between 16 March 2020 and 31 May 2021 Malaysia reported 571,901 cases and 2,796 deaths [3]. In addition, travel-related COVID-19 cases were identified. COVID-19 poses a genuine threat to all countries due to global transportation and the popularity of tourism. As this disease can spread through direct or indirect contact, the possibility of people getting infected can occur when a COVID-19 patient travels in the same transportation [4].

The outbreak of COVID-19 has inspired researchers to perform simulations of the virus spreading in airplanes [5]. For example, a study on in-flight aerosol transmission and surface contamination using an in-house developed computational model of a cabin zone of Boeing 737. This study compared aerosol transmission in three models: a model with full passenger capacity (60 passengers), a model with reduced capacity (40 passengers), and a model at full capacity with sneeze guards/shields between passengers [6].

In this study, a computationally efficient model of viral spread was utilised to better understand the influence of stochastic factors on a large-scale system such as an air traffic network [7]. A particle-based model of passengers and seats aboard a single-cabin 737-800 was developed to demonstrate the concept of tracking the propagation of a virus through an aircraft's passenger compartment over multiple flights. The model is sufficiently computationally efficient to be viable for Monte Carlo simulations to capture various stochastic effects, such as the number of passengers, number of initially sick passengers, seating locations of passengers, and baseline health of each passenger [8].

Yan *et al.*, [9] conducted a study on the transmission of COVID-19 by cough-induced particles in the cabin section of a Boeing 737 model. In each case, one passenger coughed and cough particles with measured size distributions were released and tracked using the Lagrangian framework. Horstman and Rahai [10], on the other hand, investigated virus transmission from a single infector (a passenger) in a Boeing 737-600 cabin. Their simulation used a passive scalar gas with particle sizes similar to those of influenza virus-laden particles, which were assumed to be comparable to those of coronavirus-laden particles.

Pirouz *et al.*, [11] analysed cabin airflow patterns for three types of vehicles: airplanes, buses, and cars. They created models for each vehicle type with their airplane geometry model serving as a reference for our project model development. Their study also focused on inhalation of expiratory droplets in aircraft cabins. They developed a method for predicting the number of expiratory droplets inhaled by passengers in an airliner cabin for any flight duration. The spatial and temporal distributions of expiratory droplets for the first 3 min after exhalation from the index passenger were obtained using computational fluid dynamics (CFD) simulations.

Bhatia and Santis [12] modelled the droplet dispersion after a single breath from an index patient. They conducted CFD simulations using the  $k-\omega$  SST turbulence model in ANSYS Fluent software [13]. To ensure a realistic simulation, they considered several parameters, such as the size of the mouth opening, velocity of cabin air, and number of droplets exhaled by the index patient [12]. Davis *et al.*, [14] characterised the transport of respiratory pathogens during commercial air travel. They performed simulations to track the particles expelled by coughing passengers assigned to different seats on a Boeing 737 aircraft. The simulation data were post-processed to calculate the number of particles inhaled by nearby passengers. Different airflow rates and initial conditions were used to account for random fluctuations in the flow field [14]. Bilir *et al.*, [15] numerically investigated a generic model representing airflow in a passenger cabin of a commercial airplane. The model considers half of an aircraft cabin owing to the symmetrical conditions. The airflow inside the cabin was analysed for a ceiling supply bottom return mixing ventilation system using Ansys-Fluent software [15,16].

## 2. Methodology

### 2.1 Geometry of Aircraft Cabin

A three-dimensional model of an aircraft cabin was created using the SolidWorks software. The cabin dimensions were inspired by a previous study on the numerical simulation of a novel coronavirus spread in commercial aircraft cabins. The dimensions of aircraft cabins are listed in Table 1. Figures 1 and 2 show the geometry of the aircraft cabin [7]. The purpose of constructing this cabin model is to investigate how far human breath particles travel. Therefore, only a section of the cabin and block-shaped human manikin were constructed. The cabin is designed with four inlets at the top and two outlets at the bottom.

**Table 1**  
 Model geometry of aircraft cabin

Parameter	Dimension
Length	7 m
Width	4 m
Height	2.5 m
Passenger breathing zone height	1.5 m
Inlet width	0.04 m
Outlet width	0.04 m
Passenger mouth	0.05 m
Row distance	1 m

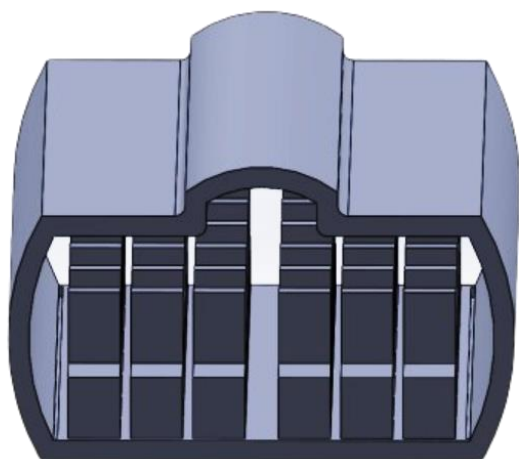


**Fig. 1.** Geometry of the aircraft cabin

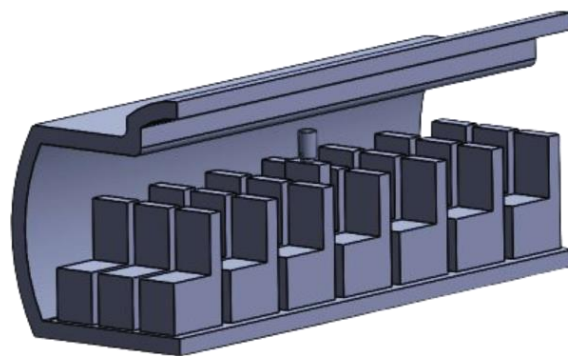


**Fig. 2.** Geometry of the cabin (section view)

### 2.2 Governing Equation

For our project, the flow characteristics and dispersion of breath and cough particles were modelled using commercial software to study the desired results. ANSYS FLUENT was used to simulate the airflow in the aircraft cabin and dispersion of breath and cough particles [18]. According to Ahmed [19], the continuity and momentum equations cannot be overlooked when accurately modelling the airflow inside an aircraft cabin.

$$\text{Continuity equation: } \frac{\partial U_i}{\partial x_i} = S_m \quad (1)$$

The source term  $S_m$  is designed to model the added mass from the discrete phase of the droplets to the surrounding air, thereby influencing the velocity vector  $U$  [20].

$$\text{Momentum equation: } \rho U_j \frac{\partial U_i}{\partial x_i} = \frac{\partial P}{\partial x_i} + \frac{\partial}{\partial x_j} \left( \mu \left[ \frac{\partial U_i}{\partial x_j} + \frac{\partial U_j}{\partial x_i} \right] - \rho \overline{u_i u_j} \right) + S_{mi} \quad (2)$$

The pressure  $P$  (Pa), viscosity  $\mu$ , and Reynolds stresses ( $u_i u_j$ ) are factors affecting the fluid dynamics, whereas ( $S_{mi}$ ) represents the sum of all body forces acting on the system.

### 2.3 Discretization of the Model

In our project, three types of mesh were generated. All meshes generated were tetrahedrons. For the first mesh, the number of grid nodes was 669,321, while the number of grid elements was 3,388,287. For the second mesh, the number of grid nodes was 723,472, while the number of grid elements was 3,676,632. For the third mesh, the number of grid nodes was 806,509, while the number of grid elements was 4,118,616. The mesh of the model shown in Figure 3 consists of 669,321 nodes and 3,388,287 elements.



**Fig. 3.** Mesh generation of the aircraft cabin model

### 2.4 Parameters and Boundary Conditions

Figures 4 and 5 present the inlet and outlet of the model, respectively. The inlet and outlet of the aircraft cabin are simplified as rectangles, whereas the inlet of the human mouth is simplified as a circle. The velocity of the aircraft inlet is set to be 1 m/s, and the inlet of the human mouth is set to be 1.3 m/s, 3.5 m/s, and 5 m/s. The pressure outlet was set to 84,475.3 Pa. Table 2 summarises the boundary conditions used in the simulations.

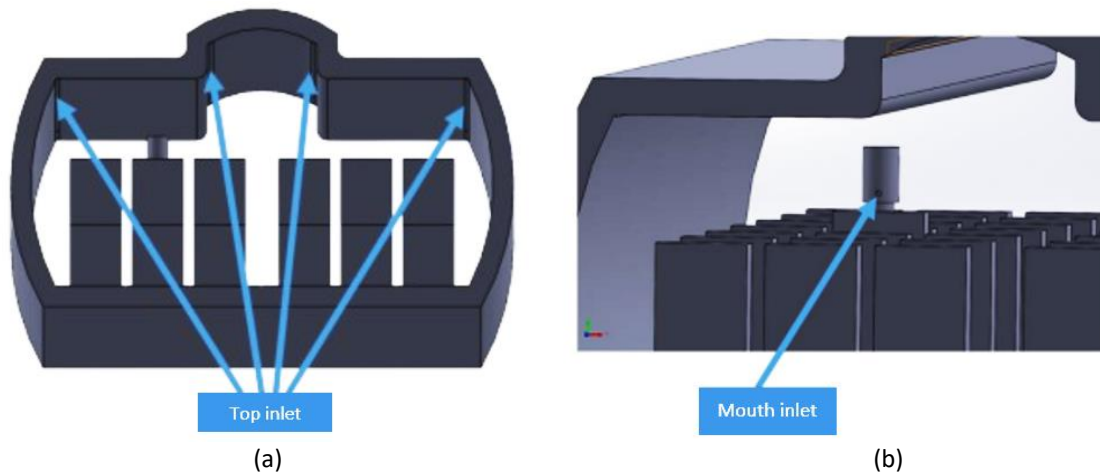


**Fig. 4.** Inlet of the aircraft cabin (a) Top (b) Mouth

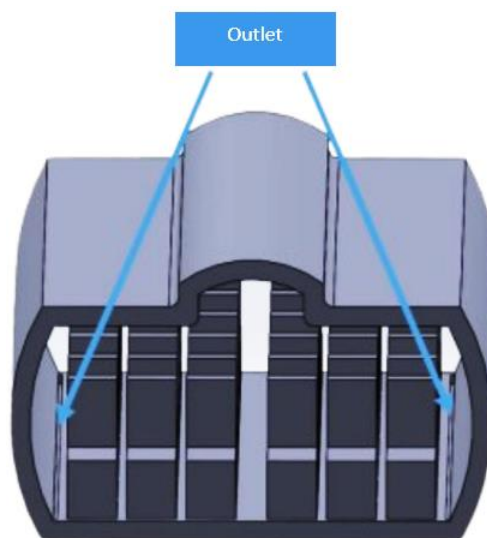


**Fig. 5.** Outlet of the aircraft cabin

**Table 2**

The boundary conditions

Distance (m)	Velocity ( $\text{ms}^{-1}$ )
Air inlet velocity	1 m/s
Mouth inlet velocity	1.5 m/s, 3.5 m/s, 5 m/s
Air outlet pressure	84475.3 Pa
Method	SIMPLE

### 3. Results

#### 3.1 Grid Independency Test

In this project, a grid independence test (GIT) was conducted to compare the mesh elements and verify the output for each mesh. The goal was to determine whether the results remained consistent despite changes in the mesh of the domains. If the results show minimal variation with different mesh sizes, we can select the minimum mesh size for the final solution output. This process helps to obtain accurate data on the velocity magnitude near the horizontal line at the mouth and to investigate the flow streamline in the aircraft cabin. The results of the velocity magnitude near the horizontal line at the mouth inlet for mesh sizes of the 669 K, 723 K, and 806 K nodes are illustrated in Figure 6.

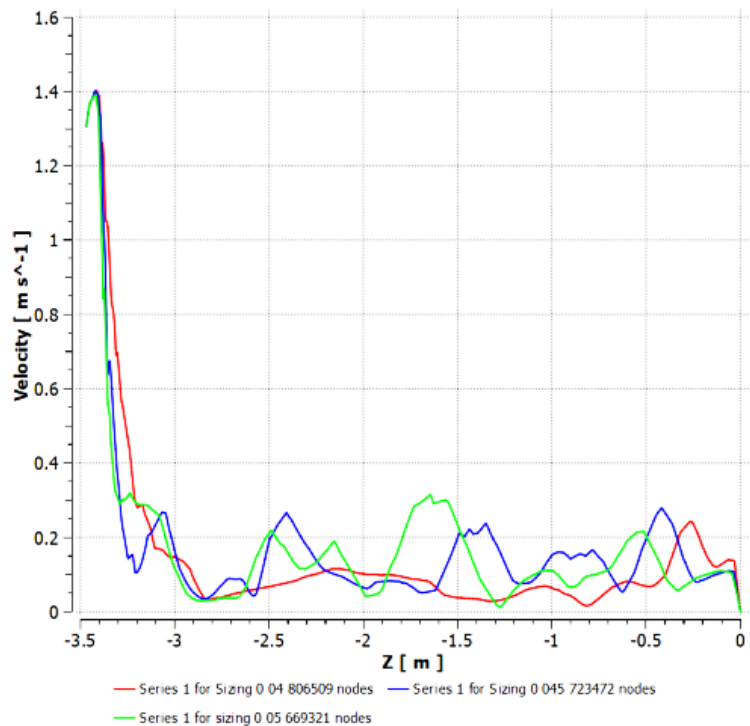


**Fig. 6.** Velocity magnitude near horizontal line of the mouth inlet with 669K, 723K, and 806K nodes

According to Figure 6, it can be observed that an increase in the number of nodes results in variations in the velocity magnitude. Unfortunately, an accurate and clear grid independence test (GIT) was not achieved for this project because the velocity magnitude still varied with an increasing number of nodes. This is attributed to the lack of powerful equipment, which limits the ability to utilise higher node meshes for the GIT. As a result, the GIT was completed only for up to 806 K nodes.

### 3.2 Result of Simulation

Table 3 presents the velocity streamlines of the breathing model at different inlet velocities of the human mouth (1.3 m/s, 3.5, and 5 m/s). The streamline patterns illustrate how air flows and mixes within an aircraft cabin. For each velocity condition, the airflow pattern changed, indicating how breath particles dispersed within the cabin. In model (A), the streamlines showed a moderate dispersion of airflow from the mouth of the patient. The airflow tended to move forward and spread out gradually, affecting the passengers seated directly in front of the patient. The dispersion pattern indicates that breath particles travel approximately 2-3 rows ahead before dissipating. In model (B), the streamlines indicate a more vigorous and broader dispersion of airflow compared to the 1.3 m/s scenario. The airflow moved forward and sideways, covering a larger area within the cabin. This higher velocity results in breath particles potentially reaching up to 3-4 rows ahead and affecting more passengers on both sides of the cabin. Model (C) shows a highly energetic dispersion, with the airflow moving rapidly forward and spreading widely. The particles dispersed further, indicating that they could affect passengers up to five rows ahead. The wider spread of airflow also suggests that more passengers on either side of the patient might be exposed to breath particles.

**Table 3**  
 Velocity streamline of the breathing of model A, B and C

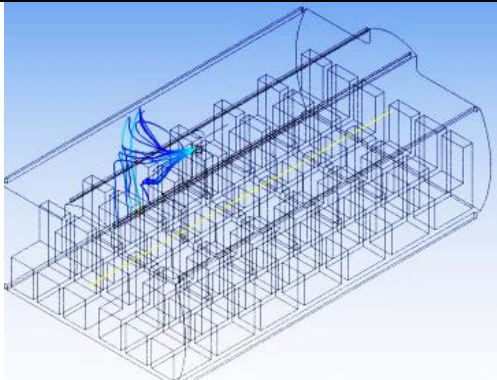
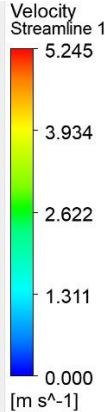
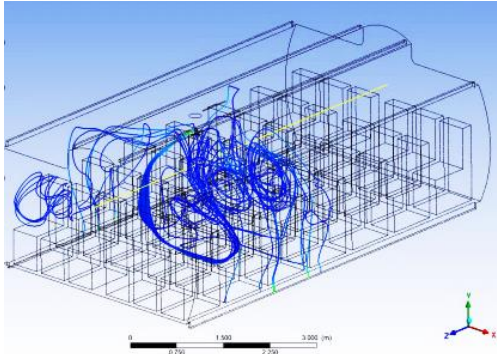
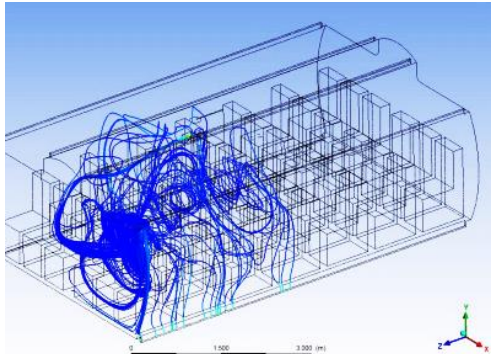
Velocity streamline	Legend	Model
1.3 m/s		 <p>Model (A)</p>
3.5 m/s		 <p>Model (B)</p>
5 m/s		 <p>Model (C)</p>

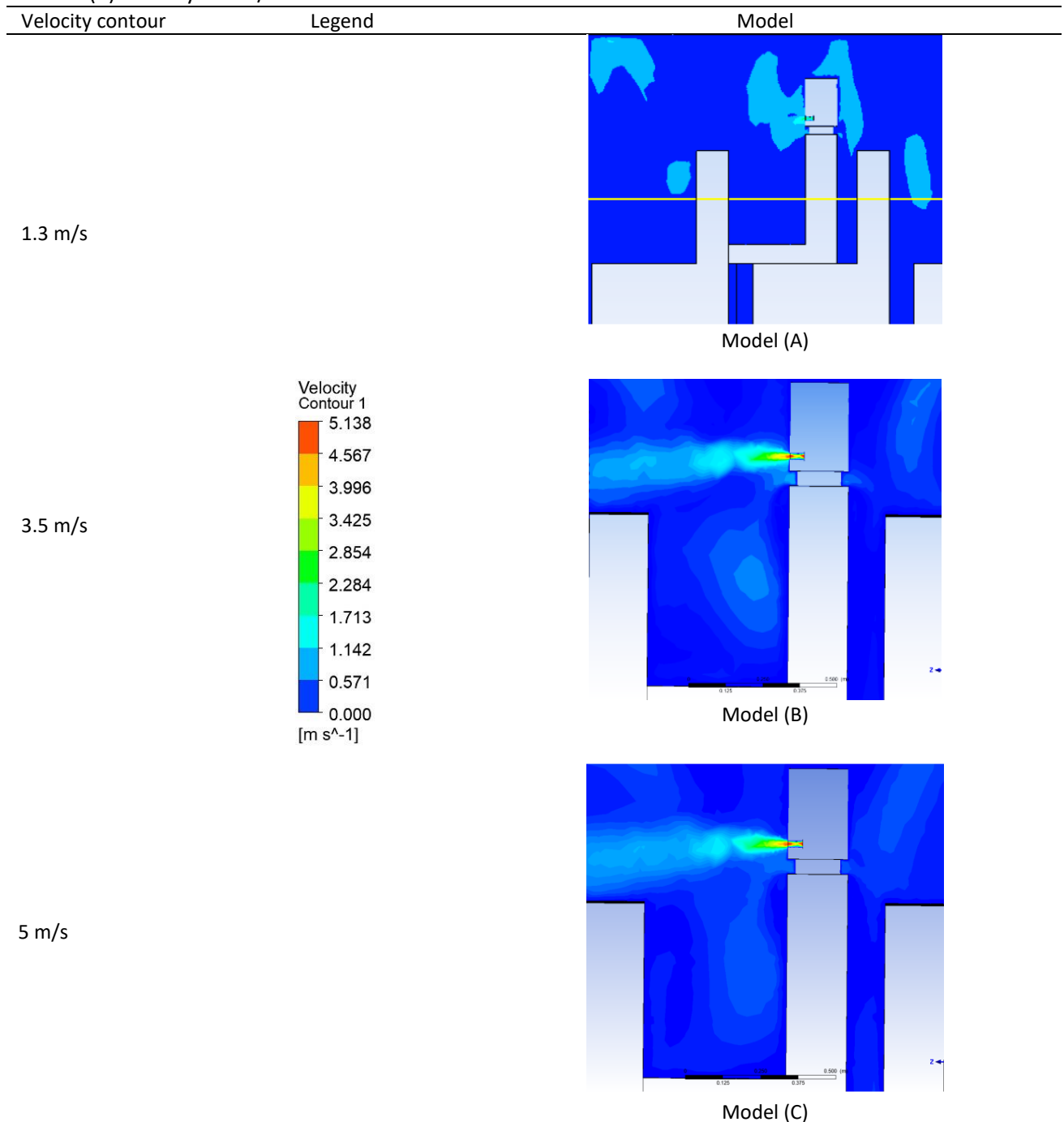
Table 4 lists the velocity contours of the breathing model for the same inlet velocity. The contour plots provide a detailed view of the velocity distribution across the cabin, indicating the areas of high and low velocities. These contours are crucial for understanding the spread and settling of breath particles in the different regions of the cabin. In model (A), the contour plot shows areas of high velocity concentrated around the mouth inlet, which gradually decreased as the distance from the patient increased. The high-velocity region was relatively small, indicating a limited dispersion of breath particles. Passengers seated immediately in front of and beside the patient were more likely to experience higher airflow velocity.

Model (B) demonstrates that the velocity contour expands significantly compared to the 1.3 m/s scenario. There was a larger region of high velocity, indicating that breath particles were dispersed more widely and with greater force. The contours suggest that passengers seated further from the

patient, both in front and to the sides, were exposed to higher velocities and potentially more breath particles. In model (C), the contour plot shows an even broader area of high velocity extending further into the cabin. The high-velocity region was extensive, covering multiple rows ahead of the patient. This scenario indicates that breath particles are dispersed with significant energy, affecting passengers located several rows away and increasing their potential exposure to airborne particles.

**Table 4**

Velocity distributions of the breathing of model (A) velocity of 1.3 m/s, model (B) velocity of 3.5 m/s and model (C) velocity of 5m/s





The analysis of Tables 3 and 4 provides insights into how the velocity of a patient's breath influences the dispersion of potentially virus-laden particles within an aircraft's cabin. It was found that higher inlet velocities resulted in a wider and more vigorous dispersion of airflow, potentially increasing the risk of exposure to other passengers. These findings emphasise the importance of implementing effective ventilation and air filtration systems in aircraft cabins to mitigate the spread of airborne pathogens and protect passenger health.

Figure 7 depicts the magnitude of the velocity near the horizontal line of the mouth inlet for three different velocities (1.3 m/s, 3.5, and 5 m/s). This figure highlights the variations in the velocity magnitude directly influenced by the breathing rate of the coronavirus patient. As the inlet velocity increased, the magnitude of the velocity near the mouth inlet also increased, demonstrating a more extensive dispersion range of breath particles. This information is essential for assessing risk areas within the cabin, where passengers may be more susceptible to inhaling virus-laden particles.

A comprehensive analysis of these tables and figures helps to understand the impact of a coronavirus patient's breath on airflow and potential virus dispersion in an aircraft cabin, providing insights into mitigation strategies to enhance passenger safety.

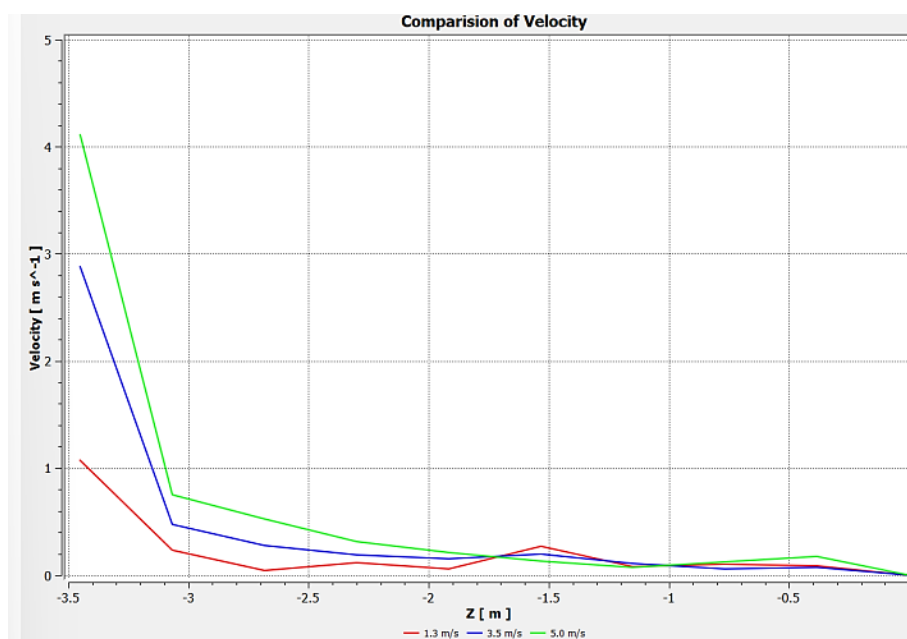


**Fig. 7.** Velocity magnitude near the horizontal line of the mouth inlet with 1.3 m/s, 3.5 m/s and 5 m/s

#### 4. Conclusions

This study demonstrated that higher inlet velocities resulted in a wider and more active dispersion of airflow, as evidenced by the simulation results. This may potentially expose passengers to each other, thereby increasing the risk of infection. At an inlet velocity of 1.3 m/s, the breath particles moved to the next 2-3 rows before dissipating. At 3.5 m/s, the particles could have reached up to 3-4 rows away from the source. At 5 m/s, the particles could impact up to five rows of passengers. These findings emphasise the importance of proper ventilation and air-conditioning systems in aircraft cabins to prevent the distribution of pathogens and protect passenger health. Future studies should consider other factors that affect breath flow characteristics, including temperature, humidity, and a wider range of velocities, to improve the models and the efficacy of interventions.

## Acknowledgement

This research was supported by Universiti Tun Hussein Onn Malaysia (UTHM) through Tier 1 (vot Q542).

## References

- [1] Huang, Chaolin, Yeming Wang, Xingwang Li, Lili Ren, Jianping Zhao, Yi Hu, Li Zhang et al. "Clinical features of patients infected with 2019 novel coronavirus in Wuhan, China." *The Lancet* 395, no. 10223 (2020): 497-506. [https://doi.org/10.1016/S0140-6736\(20\)30183-5](https://doi.org/10.1016/S0140-6736(20)30183-5)
- [2] Elengoe, Asita. "COVID-19 outbreak in Malaysia." *Osong public health and research perspectives* 11, no. 3 (2020): 93. <https://doi.org/10.24171%2Fj.phrp.2020.11.3.08>
- [3] Jayaraj, Vivek Jason, Sanjay Rampal, Chiu-Wan Ng, and Diane Woei Quan Chong. "The epidemiology of COVID-19 in Malaysia." *The Lancet Regional Health—Western Pacific* 17 (2021). <https://doi.org/10.1016/j.lanwpc.2021.100295>
- [4] Ningthoujam, Ramananda. "COVID 19 can spread through breathing, talking, study estimates." *Current medicine research and practice* 10, no. 3 (2020): 132. <https://doi.org/10.1016%2Fj.cmrp.2020.05.003>
- [5] Riquelme, Fabián, Ana Aguilera, and Alonso Inostrosa-Psijas. "Contagion modeling and simulation in transport and air travel networks during the COVID-19 pandemic: a survey." *IEEE Access* 9 (2021): 149529-149541. <https://doi.org/10.1109/ACCESS.2021.3123892>
- [6] Talaat, Khaled, Mohamed Abuhegazy, Omar A. Mahfoze, Osman Anderoglu, and Svetlana V. Poroseva. "Simulation of aerosol transmission on a Boeing 737 airplane with intervention measures for COVID-19 mitigation." *Physics of Fluids* 33, no. 3 (2021). <https://doi.org/10.1063/5.0044720>
- [7] Harolanuar, Muhammad Nur Hanafi, Nurul Fitriah Nasir, Hanis Zakaria, and Ishkrizat Taib. "Analysis of fluid flow on the n95 facepiece filtration layers." *Journal of Advanced Research in Fluid Mechanics and Thermal Sciences* 100, no. 1 (2022): 172-180. <https://doi.org/10.37934/arfmts.100.1.172180>
- [8] McCue, Leigh. "A low-fidelity stochastic model of viral spread in aircraft to assess risk mitigation strategies." *ASCE-ASME Journal of Risk and Uncertainty in Engineering Systems, Part B: Mechanical Engineering* 7, no. 3 (2021): 031002. <https://doi.org/10.1115/1.4050040>
- [9] Yan, Yihuan, Xueren Li, Xiang Fang, Ping Yan, and Jiyuan Tu. "Transmission of COVID-19 virus by cough-induced particles in an airliner cabin section." *Engineering Applications of Computational Fluid Mechanics* 15, no. 1 (2021): 934-950. <https://doi.org/10.1080/19942060.2021.1922124>
- [10] Horstman, Ray, and Hamid Rahai. "A risk assessment of an airborne disease inside the cabin of a passenger airplane." *SAE International Journal of Advances and Current Practices in Mobility* 3, no. 2021-01-0036 (2021): 1263-1271. <https://doi.org/10.4271/2021-01-0036>
- [11] Pirouz, Behrouz, Domenico Mazzeo, Stefania Anna Palermo, Seyed Navid Naghib, Michele Turco, and Patrizia Piro. "CFD investigation of vehicle's ventilation systems and analysis of ACH in typical airplanes, cars, and buses." *Sustainability* 13, no. 12 (2021): 6799. <https://doi.org/10.3390/su13126799>
- [12] Bhatia, Dinesh, and Antonio De Santis. "A preliminary numerical investigation of airborne droplet dispersion in aircraft cabins." *Open Journal of Fluid Dynamics* 10, no. 3 (2020): 198-207. <https://doi.org/10.4236/ojfd.2020.103013>
- [13] Abd Rahman, Muhammad Faqhrurrazi, Norzelawati Asmuin, Nurul Fitriah Nasir, Ishkrizat Taib, Mohamad Nur Hidayat Mat, and Riyadhthusollehan Khairulfuaad. "Effect of Different Orifice Diameter on The Flow Characteristic in Pressurized Metered Dose Inhaler by Using CFD." *CFD Letters* 12, no. 3 (2020): 39-49.
- [14] Zee, Malia, Angela C. Davis, Andrew D. Clark, Tateh Wu, Stephen P. Jones, Lindsay L. Waite, Joshua J. Cummins, and Nels A. Olson. "Computational fluid dynamics modeling of cough transport in an aircraft cabin." *Scientific reports* 11, no. 1 (2021): 23329. <https://doi.org/10.1038/s41598-021-02663-8>
- [15] Bilir, Levent, Hasan Çelik, and Mehmet Barış Özerdem. "Investigation of Air Flow Inside an Airplane Passenger Cabin." *Turkish Journal of Materials* 6, no. 2 (2021).
- [16] Kareem, Ali Kamil, Adian H. Al-Mozan, Safaa Abbood Kadhim, Maedah A. Al-Birmani, I. R. Ali, A. E. Ismail, and Ishkrizat Taib. "Design and manufacture a dust sensing device to monitor breathing air." In *AIP Conference Proceedings*, vol. 2955, no. 1. AIP Publishing, 2023. <https://doi.org/10.1063/5.0181664>
- [17] Zhang, Mengya, Nu Yu, Yao Zhang, Xin Zhang, and Yu Cui. "Numerical simulation of the novel coronavirus spread in commercial aircraft cabin." *Processes* 9, no. 9 (2021): 1601. <https://doi.org/10.3390/pr9091601>
- [18] Rajendran, Rahul R., Florin Emilian Țurcanu, Rahman Tawfiqur, and Homayoun Askarpour. "Computational fluid dynamic analysis of corona virus patients breathing in an airplane." *Physics of Fluids* 35, no. 3 (2023). <https://doi.org/10.1063/5.0139733>

- [19] Mboreha, Chanfiou Ahmed, Xavier Tytelman, Collins Nwaokocha, Abayomi Layeni, Ruth C. Okeze, and Abdalah Shaibu Amiri. "Numerical simulations of the flow fields and temperature distribution in a section of a Boeing 767–300 aircraft cabin." *Materials Today: Proceedings* 47 (2021): 4098-4106. <https://doi.org/10.1016/j.matpr.2021.06.426>
- [20] Azam, Syafiqah Ruqaiyah Saiful, Shaiful Fadzil Zainal Abidin, Izuan Amin Ishak, Amir Khalid, Norrizal Mustaffa, Ishkrizat Taib, Safra Liyana Sukiman, and Nofrizalidris Darlis. "Flow Analysis of Intake Manifold Using Computational Fluid Dynamics." *International Journal of Integrated Engineering* 15, no. 1 (2023): 88-95. <https://doi.org/10.30880/ijie.2023.15.01.008>